Available online at www.sciencedirect.com
ScienceDirect
Polymer 49 (2008) 1812–1822
polymer
www.elsevier.com/locate/polymer

Spectroscopic studies and first-principles modelling of 2,2,4-trifluoro-5-trifluoromethoxy-1,3-dioxole (TTD) and TTD–TFE copolymers (Hyflon® AD)

Alberto Milani [a,*], Matteo Tommasini [a], Chiara Castiglioni [a], Giuseppe Zerbi [a], Stefano Radice [b], Giorgio Canil [b], Paolo Toniolo [b], Francesco Triulzi [b], Pasqua Colaianna [b]

[a] *Dipartimento di Chimica, Materiali e Ingegneria Chimica, ''G. Natta'', Politecnico di Milano, Piazza Leonardo da Vinci, 32, 20133 Milano, Italy*
[b] *Solvay Solexis Research and Technology, Viale Lombardia 20, 20021 Bollate (MI), Italy*

Received 20 December 2007; received in revised form 25 January 2008; accepted 28 January 2008
Available online 10 February 2008

Abstract

Amorphous fluorinated optical polymers, characterized by high transparency in the visible and near infrared spectra, high glass transition temperature and very good resistance to chemical environment, have been developed by co-polymerisation of tetrafluoroethylene (TFE) and 2,2,4-trifluoro-5-trifluoromethoxy-1,3-dioxole (TTD). In this work we study at molecular level the effect of the introduction of the bulky TTD unit in a perfluoroalkyl chain.

In particular the effect on the molecular structure and chain flexibility is investigated and spectroscopic markers correlated to chemical and structural defects are identified. The study includes a thorough experimental spectroscopic analysis (infrared and Raman spectra) of several different copolymer samples and a modelling based on Density Functional Theory calculations and semiempirical calculations on suitable model molecules.

Keywords: Fluorinated polymers; Vibrational spectroscopy; First-principles calculations

1. Introduction

The recent technologies intertwined with communication devices, electronics and optics require the development of new materials with outstanding chemical, optical and mechanical properties. Among organic polymers, materials based on perfluoropolymers provide the ultimate resistance to hostile chemical environments (such as acids and alkalis, fuels and oils, low molecular weight esters, ethers and ketones, aliphatic and aromatic amines and strong oxidizing substances) and high working temperatures. In the field of optical applications, different kinds of monomers, polymers and copolymers have been proposed and new ones are constantly synthesized [1–16]. In this paper, we deal with a family of copolymers of tetrafluoroethylene (TFE) and 2,2,4-trifluoro-5-trifluoromethoxy-1,3-dioxole (TTD), known commercially as Hyflon® AD. They are amorphous perfluoropolymers with a glass transition temperature (T_g) significantly higher than the room temperature. Moreover, they show thermal decomposition temperatures exceeding 400 °C [16–18].

In Fig. 1 the route of TTD synthesis is illustrated [18,19].

The refractive index of the homopolymer of TTD matches that of water: it follows that when a sample is immersed in water it becomes invisible.

Depending on their composition, copolymers span a refractive index range from 1.32 to 1.331. These values make them suitable for many optical applications: for instance it is possible to obtain optical fibers with high values of numerical aperture, a characteristic which allows to have a good signal launch into the fibers. Moreover, TTD–TFE copolymers are

* Corresponding author. Tel.: +39 0223993383; fax: +39 0223993231.
E-mail address: alberto.milani@polimi.it (A. Milani).

0032-3861/$ - see front matter © 2008 Elsevier Ltd. All rights reserved.
doi:10.1016/j.polymer.2008.01.072

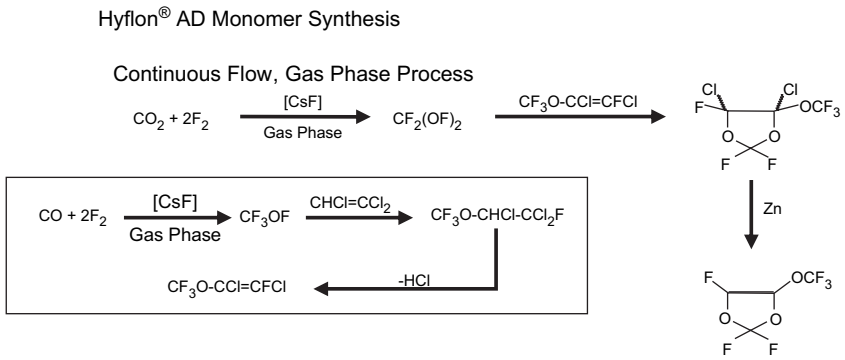

Fig. 1. Sketch describing the synthesis of 2,2,4-trifluoro-5-trifluoromethoxy-1,3-dioxole (TTD).

transparent from deep UV to near infrared: in a plastic optical fiber (POF) made with this material, a signal can be transmitted for several kilometers without needing any amplification. Thanks to its transparency in the deep UV it is possible to use Hyflon® AD as a material for protective pellicles in the manufacturing of semiconductors [20].

In addition to these peculiar characteristics, we should also mention its ability to decrease the reflectance of an LCD screen: a layer of Hyflon® AD with a thickness of just half a micron lowers the reflectivity by 80%.

All the optical applications described above require that the occurrence of contaminants, either suspended or dissolved in the polymer solution, has to be carefully avoided by means of suitable purification process [21].

The peculiar properties and the great number of possible applications make this class of amorphous materials a candidate for state of the art technology in different fields such as optics, photonics, electronics, membrane science, biotechnology, nanotechnology.

In the present paper we will study the molecular structure of TTD monomer and of the TTD–TFE copolymers in order to find correlations between the outstanding macroscopic properties and the molecular structural parameters.

This work is based on both experimental and theoretical tools: namely vibrational spectroscopy, quantum chemical simulations and modelling.

2. Experimental

InfraRed (IR): mid-infrared (4000–400 cm^{-1}) spectra of solid samples of the polymer were recorded with a Nicolet Nexus FT-IR spectrometer; each spectrum was acquired by accumulating 256 scans at 2 cm^{-1} of resolution. Gas phase spectra were recorded with a Nicolet Nexus 870 spectrometer (2 cm^{-1} resolution, 256 scans), using a gas sample cell with an optical path length of 10 cm; the relative pressure of the samples was of the order of 10^{-2} mbar.

NIR: Near IR (11 000–3000 cm^{-1}) spectra were recorded with a Nicolet Nexus 870 spectrometer equipped with near IR optics (CaF_2 beamsplitter, PbSe detector); 512 scans were accumulated, with a resolution of 2 cm^{-1}.

FIR: Far IR (650–100 cm^{-1}) spectra were recorded with a Nicolet Magna 850 FT-IR spectrometer equipped with far optics (solid-substrate beamsplitter for FIR and a polyethylene windowed DLaTGS detector); 256 scans were accumulated, with a resolution of 4 cm^{-1}.

Raman and FT-Raman spectra were recorded with a Dilor XY Raman spectrometer using as exciting line the 514.5 nm of a Kr–Ar Spectra Physics laser: typical power on the sample was of the order of 100 mW. FT-Raman spectra were recorded with a Thermo Nicolet FT Raman module linked to Nicolet Nexus 870 spectrometer; the resolution was 4 cm^{-1} or 8 cm^{-1} and according to S/N ratio the number of scans ranged from 512 to 16 384. The exciting line was in the near infrared at 1064 nm; power on the sample was usually in the range 200–300 mW.

3. Relevant optical properties

As already discussed in Section 1, one of the relevant properties that makes a material suitable for optical communications is its high degree of transparency in the spectral region commonly used for the transmission of optical signals. In addition to the need of purification from the contaminants [21], this requirement can be fulfilled if we guarantee that the material is fully amorphous and if transitions giving absorption in the spectral region of interest are absent for the polymer.

In spite of the fact that many amorphous polymers show very high energy gaps between the ground and the first excited electronic states, the intrinsically weak transitions associated to vibrational overtones or combination bands make them unsuitable for the transmission of optical signals for long distances.

In this respect, materials like perfluorinated polymers are the best candidates since their overtones and combination bands are displaced from those of polymers containing CH bonds [22]. This property makes the frequency range used in optical communications free from relevant absorptions.

3.1. Absorption transitions in the near infrared spectral region

In Fig. 2 the NIR spectra of the homopolymer are compared with the spectrum obtained from a sample of polymethyl methacrylate (PMMA) of comparable thickness (about 5 mm). Although the spectra were recorded on a relatively

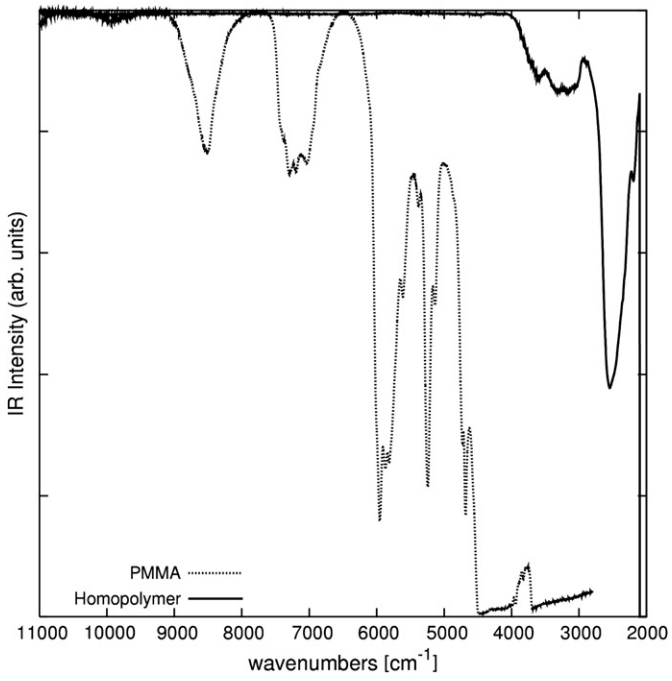

Fig. 2. Comparison between NIR spectra of polymethylmethacrylate (dashed) and TTD homopolymer (solid).

thin sample, we expect that also for very thick samples the absorptions in the NIR frequency range remain very weak, thus obtaining a good transmission of optical signals in this frequency range. This becomes evident if we make a comparison with the hydrogenated polymers that are commonly used for optical applications: the fundamental vibrations in fluorinated polymers are generally observed at wavenumbers below 1400 cm^{-1}, while hydrogenated systems show strong bands due to CH stretching vibrations near 3000 cm^{-1}. Therefore in the relevant spectral range (common transmission lines in the NIR are at 1.55 μm and 1.31 μm, i.e. at 6451 cm^{-1} and 7633 cm^{-1}, respectively), the perfluorinated polymers will show absorptions associated to 5th or 6th overtones while the 2nd or 3rd ones appear in the spectrum of the hydrogenated ones. Independently from the chemical species involved in the vibrational transition, it is well known [23,24] that a dramatic decrease of the absorption intensity is expected upon increasing the order of the overtone. Therefore, this fact accounts for the lack of a significant absorption in the range of interest for perfluorinated polymers.

3.2. Crystal phases

Chemical and structural regularities of the polymer chain are required in order to obtain semicrystalline materials. This implies that the first control of the microstructure and morphology takes place at the level of the polymer synthesis.

The polymerisation reaction followed for the synthesis of the TTD homopolymer does not allow a control of the head-to-tail or head-to-head linking of the monomer units. Moreover, at least in principle, the CC bonds that link the rings can take both *anti* or *syn* configuration (see the sketch in Fig. 4). As a consequence, it is very unrealistic to expect that even short sequences of structurally ordered units could be obtained. On the other hand, the bulky cyclic unit that forms the homopolymer hinders for kinetic reasons the occurrence of a regular conformation (and hence of crystalline domains), even in those cases where sequences with regular configuration are present. The latter peculiarity is one of the reasons why also in the case of copolymers with long CF_2 sequences we expect the introduction of TTD units to reduce the ability to form crystalline domains.

On this basis, we can safely state that in the case of the homopolymer a glassy, fully amorphous material is obtained.

The case of the copolymers is a partially open question: indeed, depending on the relative amount of TTD and TFE, the possible occurrence of long sequences of CF_2 units, prone to segregate into crystalline domains, has to be taken into account.

This observation provides a strong motivation for the research of reliable spectroscopic markers of the presence of conformational disorder in the TFE chains of the copolymers. On the other hand, a model to estimate the perturbation induced by the TTD units on the structure of the CF_2 sequences would be a valuable tool for the understanding of the properties of the copolymers. This task will be accomplished through the theoretical approach presented in Section 4.2.

3.3. Spectroscopic markers of conformational disorder

In the FIR spectral range (100–400 cm^{-1}), the normal vibrational modes characteristic of inorganic materials (as far as heavy atoms are involved), collective skeletal normal modes and out-of-plane deformations of organic polymers and molecules are usually observed. Also in the case of polytetrafluoroethylene (PTFE) the analysis of bands in this spectral region can give indications on the chain conformation.

PTFE fundamental transitions have been assigned to the suitable $q = 0$ phonons of the regular helical chain conformations, according to the predicted phonon dispersion curves [25].

The thermodynamically stable chain at room temperature has a 15/7 helical structure, in agreement with the crystal structure obtained by X-ray diffraction [26]. However, other regular conformations corresponding to relative minima of the intramolecular potential energy of the chain have been theoretically predicted and the corresponding different crystal modifications have been experimentally investigated [26]. While a 3D crystalline domain necessarily requires a regular helical conformation of the single chain, in the semicrystalline material many polymer chains pass through an amorphous phase, with disordered conformations. Spectroscopic studies were developed in order to find a parameter somehow related to the conformational ''order/disorder'' ratio [27–30]. The most popular one is the one that was proposed by Moynihan [27] and it is based on the measurement of the relative optical densities in the mid-infrared spectrum at 778 cm^{-1} and 2365 cm^{-1}. The first band has been assigned to normal modes characteristic of chain conformations different from the 15/7 helix and is considered as a marker of conformational ''disorder''. The second band at 2365 cm^{-1} is structured and broad and it is assigned to overtones and

combinations related to CF and CC stretchings; it is simply used as a normalization factor.

Another marker of conformational disorder can be identified by studies on polytetrafluoroethylenes containing chemical defects, as, for instance, copolymers obtained by the addition of a co-monomer different from TFE. The occurrence of a chemical defect in the PTFE chain induces local disorder and can also perturb the equilibrium conformation (15/7 helix) to various extent. This depends on the relative amount and on the chemical structure of the co-monomer. Normal mode analysis [25,31] indicates that it is possible to evaluate the degree of disorder through the intensity ratio (R_{FIR}) between the FIR bands observed at 293 cm^{-1} and 277 cm^{-1}.

The band at 293 cm^{-1} is assigned to the Longitudinal Optical (LO) $q = 0$ phonon corresponding to the E_1 fundamental transition of the 15/7 helix (regularity band) and its intensity is assumed to be proportional to the amount of conformational "order" [25]. The intensity of the band at 277 cm^{-1} (assigned to vibrational modes of conformationally distorted chains [25]) increases together with the amount of the co-monomer, thus giving an estimate of the degree of perturbation due to the defects. Since the marker band at 277 cm^{-1} has been assigned to vibrations of the "perturbed" $(CF_2)_n$ (from studies on PTFE samples), the measure of R_{FIR} can be used for diagnostic purposes only when the co-monomer content is relatively low, namely a few % mol.

On the other hand, the study of the FIR region could be useful whenever relevant bands in the mid-infrared are blurred by other transition characteristics of the monomer/polymer. We found a good sensitivity for the R_{FIR} parameter, in the case of TFE/TTD copolymers in a compositional range 0.5–2% mol (semicrystalline polymers, whose synthesis is described in Ref. [32]). The results indicate that the TTD monomer is very effective in inducing conformational disorder. As already pointed out, this is a simple method to prevent crystallinity in the polymeric material.

In Fig. 3 FIR spectra are reported for some copolymer samples with increasing percentage of TTD: besides the 277 cm^{-1} band, which shows a clear increase in intensity when the amount of the co-monomer increases, a component at about 390 cm^{-1} is observed. This band is characteristic of the dioxole co-monomer and can also be used as an analytical marker. The R_{FIR} parameter approach has been applied also to polymers with different kinds of "perturbing" co-monomers, such as perfluoromethyl vinyl ether (MVE) and perfluoropropyl vinyl ether (PVE), added in a similar amount as the dioxole (see Table 1 for details). We have always observed that the induced disorder is larger when the TTD monomer is present, a fact that confirms the capability of the dioxole unit to hinder the formation of conformationally ordered TFE segments.

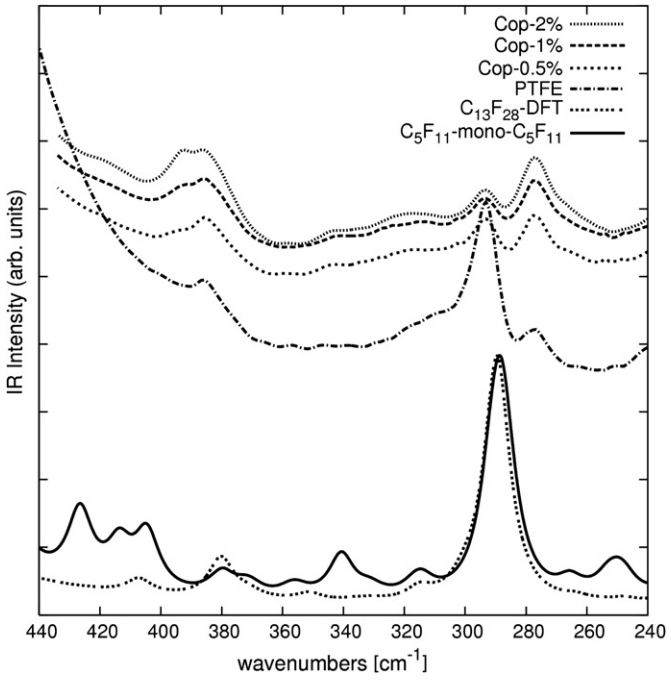

Fig. 3. Top: FIR spectra of PTFE and three TFE–TTD copolymers with different contents of TTD. Bottom: comparison between the simulated B3LYP/6-311G** FIR spectra of a short TFE chain and the model for TFE–TTD copolymer (see Section 4).

Table 1
Comparison of experimental R_{FIR} parameter for PTFE and TFE copolymers with increasing amount of TTD comonomers or comonomers of different kind

Sample	% Co-monomer	R_{FIR}
PTFE	0	5
1	TTD: 1.8	0.35
2	TTD: 1	0.51
3	TTD: 0.5	0.82
4	TTD: 0.1	2
	MVE: 2.4	0.4
	PVE: 1.4	0.6

4. Theoretical modelling

In this section the results of theoretical predictions on model molecules are illustrated for the following aims:

(1) to support the interpretation of the spectroscopic experimental data through simulation of the spectra, normal mode analyses and band assignment;

(2) to discuss the effect of the presence of TTD monomer on the structure and on the flexibility of the chain.

Calculations were carried out at different levels:

A DFT calculations

Small molecules were described through Density Functional Theory (DFT) calculations. Due to its well known performances for prediction of vibrational spectra, we have chosen B3LYP functional [33] with 6-311G** basis set. The molecules we considered are illustrated in Fig. 4: (i) TTD monomer; (ii) a very naïve model of the chemical unit of the homopolymer, namely a "reacted" monomer with two CF_3 end groups. Two different configurations were considered, corresponding to *anti* and *syn* substitutions; (iii) a model of the copolymer, represented by one TTD unit linked to two $(CF_2)_4$–CF_3 chains. Also in this case the two configurations (*anti* and *syn*) were considered; (iv) an oligomer, namely $CF_3(CF_2)_{11}CF_3$, as a model of PTFE.

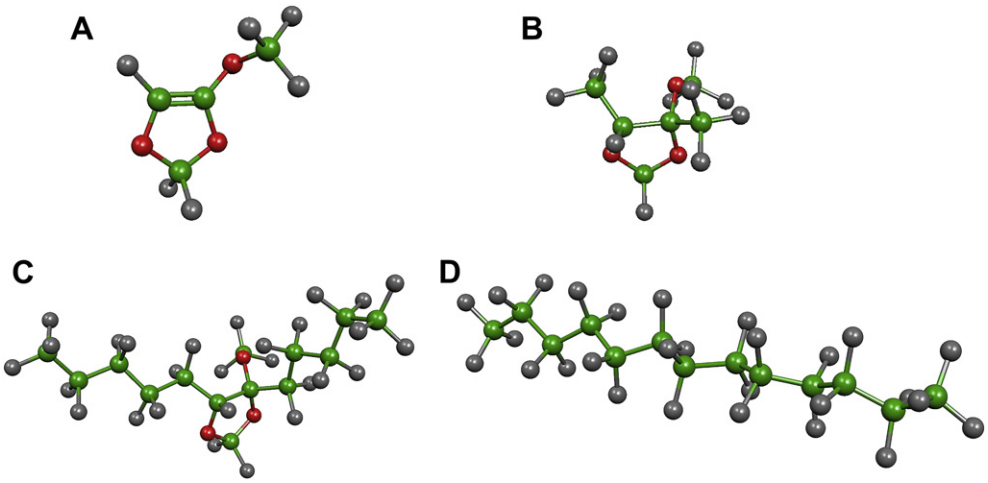

Fig. 4. Sketch of the model molecules studied: (i) TTD monomer; (ii) the ''reacted'' TTD monomer (*anti* configuration); (iii) a model for the co-polymer unit; (iv) a PTFE oligomer ($C_{13}F_{28}$) (see text).

For all these molecules IR and Raman spectra have been compared with the available experimental spectra.

B Semiempirical AM1 calculations

Other molecular models of the copolymer were studied through a semiempirical AM1 method [34]. This study is aimed at an investigation of the different stable conformations of model molecules, with the purpose of clarifying the effect of the introduction of a TTD unit on the degree of flexibility of a PTFE chain.The models studied are: (i) the oligomer $CH_3(CH_2)_{31}CH_3$ taken as model of a very flexible polyethylene (PE) chain; (ii) the oligomer $CF_3(CF_2)_{31}CF_3$ taken as model of an ''unperturbed'' PTFE chain (sketched in Fig. 5a); (iii) a model of copolymer made by a TTD unit linked to two $(CF_2)_{10}CF_3$ chains (sketched in b and c); (iv) a model of copolymer made by a $CFOCF_3$ unit linked to two $(CF_2)_{10}CF_3$ chains (sketched in d).

4.1. DFT spectra simulations

4.1.1. TTD monomer

In Fig. 6 we report the IR and Raman spectra of the monomer as predicted by DFT simulations. The experimental IR spectrum is also reported in order to give an idea of the reliability of the theoretical prediction.

Even if the computed spectrum shows an overall agreement with the experiments, showing a group of six very strong bands in the region 1180–1400 cm^{-1}, the experimental features are not very well reproduced in detail. The main discrepancy is found in the lower frequency transitions, i.e. the pair of bands predicted at 1160 cm^{-1} and 1206 cm^{-1}; they can be correlated with the broad feature showing a maximum at 1190 cm^{-1} and its shoulder at about 1202 cm^{-1}. The overestimation of the frequency splitting of the two lines could be attributed to an inaccurate description of dynamical couplings, an effect that often occurs in the description of normal modes lying in a close energy range.

The triplet of lines observed at 1240 cm^{-1}, 1276 cm^{-1} and 1304 cm^{-1} can be correlated to the four transitions calculated at 1230 cm^{-1}, 1259 cm^{-1}, 1291 cm^{-1}, and 1308 cm^{-1}. Indeed, we may assume that, since the higher frequency doublet of the experimental spectrum shows a broad shape, it hides the three higher frequency transitions predicted by the theory. According to the computed eigenvectors associated to the transitions in the range 1200–1300 cm^{-1} we can relate them to collective vibrations involving CO stretchings, CF stretchings and bendings.

As for the weaker feature at about 1400 cm^{-1}, it is nicely reproduced (both in frequency [1398 cm^{-1}] and in relative intensity) by the simulation. In the region at wavenumbers higher than 1400 cm^{-1} the experimental spectrum is substantially flat, in agreement with calculations: these give just one very weak transition at 1887 cm^{-1}, due to the weakly IR-active stretching of the C=C double bond. A closer look at the experimental spectrum indeed reveals a very weak and broad feature at 1851 cm^{-1}.

Regarding the Raman spectra, due to the low symmetry (C_1 point symmetry group) of dioxole, transitions at the same frequencies as in the IR can be found. The very strong C=C stretching line at 1887 cm^{-1} dominates the Raman spectrum, while transitions associated to normal modes involving polar bonds (e.g. CF, CO stretchings,…) appear as weaker lines. Unfortunately the experimental Raman spectrum of TTD monomer is not yet available.

An interesting observation can be made about the frequency position of CC stretching band, in agreement with previous works on fluorinated molecules [35]: the C=C stretching frequency of the double bond is substantially higher as compared, for instance, to the CC stretching frequency of ethylene ($\nu_{CC} = 1650\ cm^{-1}$). This means that its strength is significantly increased, thus indicating that the injection of electronic charge from the lone pairs of fluorine atoms to the bonding π orbital is very efficient [35].

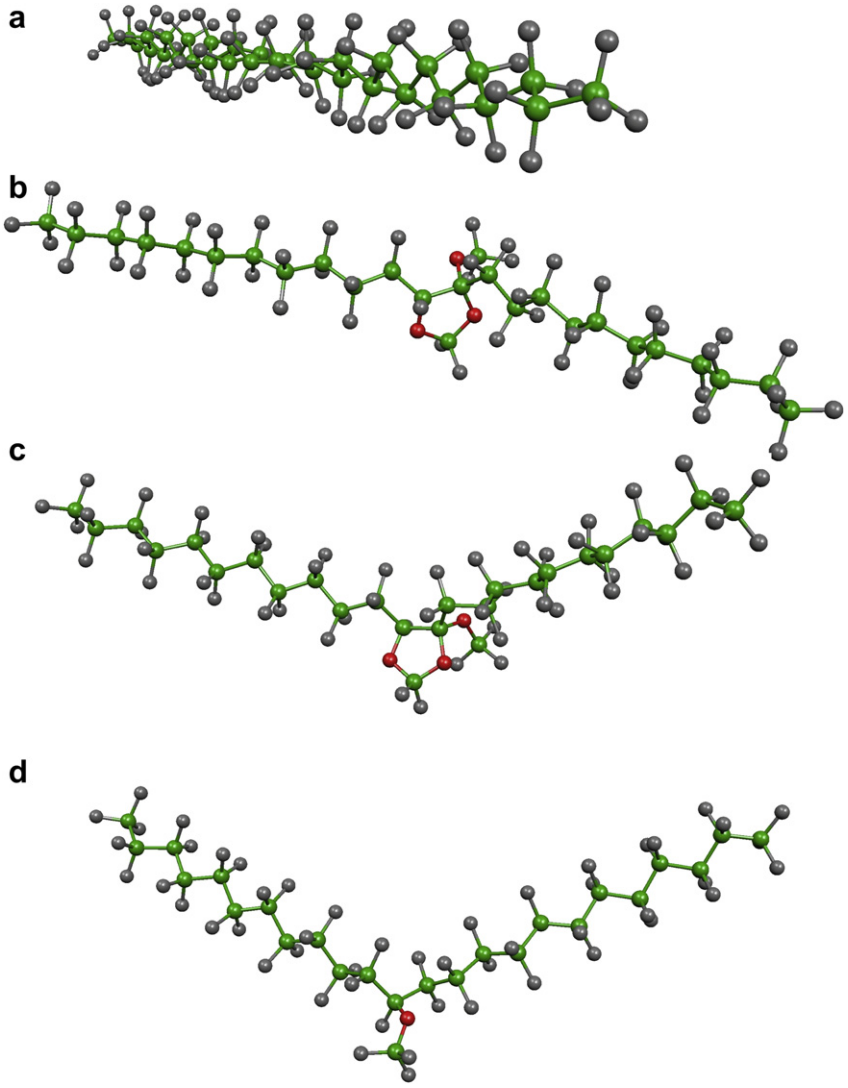

Fig. 5. Sketches of the structure of the models studied for (a) PTFE chain; (b) TTD–TFE copolymer (*anti* configuration); (c) TTD–TFE copolymer (*syn* configuration) and (d) MVE–TFE copolymer in their lower energy stable conformations, as obtained by AM1 calculations (see text).

4.1.2. Homopolymer

In Figs. 7 and 8 the DFT simulated vibrational spectra of TTD homopolymer are compared with the experimental ones.

The spectra have been calculated for the simplified model of the ''reacted'' dioxole (Fig. 4(ii)). In order to avoid couplings between the vibrations of the ring and those localized on the CF_3 end groups (obviously absent in the homopolymer) we have calculated the spectra on a fictitious isotope where the real masses of atoms belonging to the CF_3 end groups are substituted with masses of 100 amu. In this way, the characteristic vibrations of this groups are displaced at low frequency (bands in the theoretical spectra below 500 cm^{-1}, see Fig. 7) and do not perturb normal vibrations of the ring.

A look at Figs. 7 and 8 indicates that the model, in spite of its simplicity, is suitable for the prediction of the main experimental features. The comparison between the spectra calculated for two different model molecules (with *syn* and *anti* configurations of the CF_3 end groups) shows that both IR and Raman spectra are sensitive to *syn* or *anti* substitution. On this basis, it is possible to identify markers of the configuration.

While the relatively broad features observed in the IR spectrum seem to suggest that in a real sample both *syn* and *anti* configurations occur, a closer inspection of the Raman spectrum and in particular the relative intensities of the two lines in the doublet at about 900 cm^{-1} indicates that the *anti* configuration is preferred. The normal mode associated to the line at lower wavenumbers (880 cm^{-1} for the *anti* form and 915 cm^{-1} for the *syn* form) involves CO and CF stretching of the $COCF_3$ group, coupled with vibrational displacements of the nearby atoms of the ring. Since the different configurations clearly affect the environment of this group of atoms, this band is expected to be sensitive to the molecular configuration.

The same conclusion can be drawn from the shape of the experimental Raman line at about 323 cm^{-1}: it shows a second component as a shoulder on the high frequency side, which closely resembles the band shape obtained by spectra simulation for the *anti* species.

As for the complex structure (three peaks) of the Raman band observed at about 700 cm^{-1}, the comparison with the theoretical predictions of the spectra shows that they are not able to fully

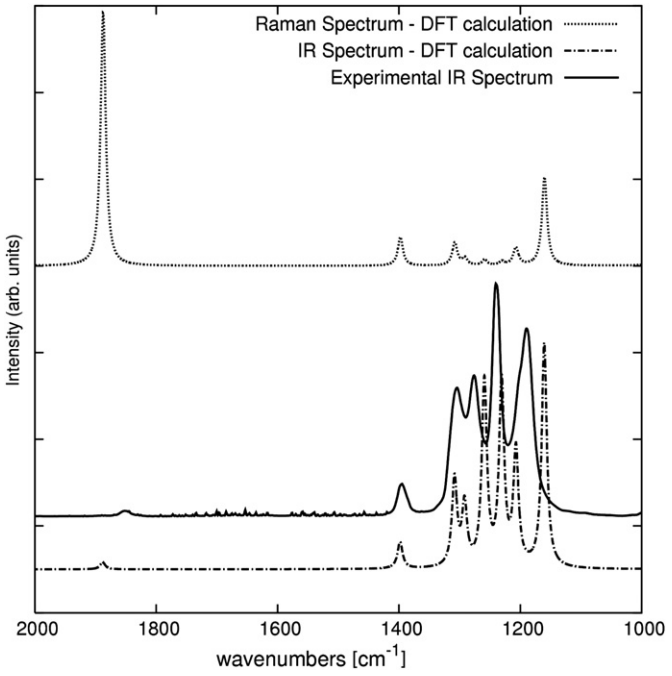

Fig. 6. Comparison between experimental and simulated (B3LYP/6-311G**) IR spectrum of the cyclic monomer (TTD) (bottom); simulated Raman spectrum of TTD monomer (top).

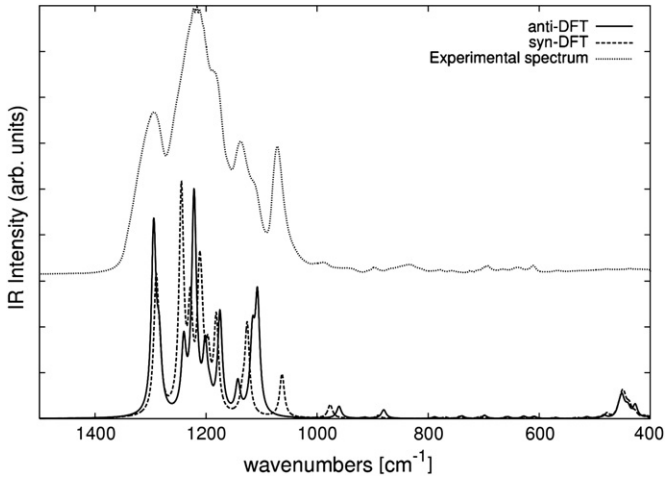

Fig. 7. Comparison between simulated (B3LYP/6-311G**) IR spectrum of ''reacted'' TTD and the IR spectrum of the TTD homopolymer.

account for the observed band shape. However, according to DFT simulations on the same model molecules with different equilibrium conformations of the pendant OCF_3 group (not shown here), we verified that the theoretical spectra of the different conformers show relevant differences in the region at around 700 cm^{-1}, thus demonstrating that the experimental features are originated by different conformations of OCF_3 group.

4.1.3. Copolymers

Spectroscopic investigations of TTD–TFE copolymers have been carried out with the following aims:

(a) To give an experimental determination of the relative abundance of TTD and TFE units in the polymer chain (this can be easily obtained if spectroscopic markers of the ring are detected).
(b) To discuss the effect of the introduction of the cyclic TTD units on the structure (e.g. conformation) of the CF_2 sequences. This is possible only if suitable markers of conformationally ordered and disordered CF_2 chains are considered (see Section 3.3).

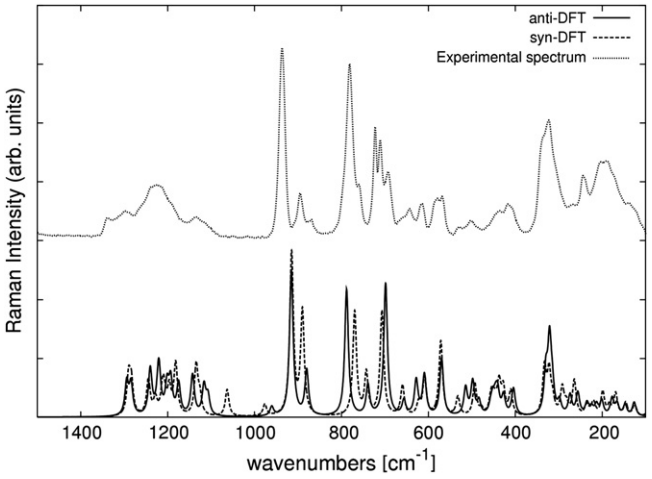

Fig. 8. Comparison between simulated (B3LYP/6-311G**) Raman spectrum of ''reacted'' TTD and experimental Raman spectrum of TTD homopolymer.

In Fig. 9 we report the experimental spectra obtained for two different random copolymers with high content of the TTD unit (molar content of 30% and 50%). These spectra are compared with the simulations on the model molecule illustrated in Fig 4(iii) that represents a dioxole unit in an environment that mimics the link with two CF_2CF_2 units. For obvious reasons the model molecule has been end-capped with two CF_3 groups.

For the sake of comparison we have also computed the vibrational spectra for a short TFE chain (11 CF_2 units). The simulations are compared to the experimental spectrum of a PTFE sample.

From Fig. 9a we immediately realize that many vibrational transitions of our model copolymer are superimposed to the absorption bands characteristic of a perfluorinated chain. However, two groups of bands outside this region can be identified as transitions involving the dioxole ring. These bands (namely at 1281 cm^{-1}, 1288 cm^{-1} and a group of five lines between 1075 cm^{-1} and 1122 cm^{-1}, as theoretically predicted) are markers of the presence of TTD units. These assignments have been verified by the analysis of the computed eigenvectors, showing vibrational displacements localized on the dioxole unit.

The predicted frequencies mentioned above can be nicely put in correspondence with the structured experimental band at 1290 cm^{-1} and with the broad feature with maximum at 1070 cm^{-1}, that indeed shows an increasing intensity trend when the percentage of TTD is increased.

As for the Raman spectrum, we can identify two well defined markers of TTD: the line predicted at 763 cm^{-1} and

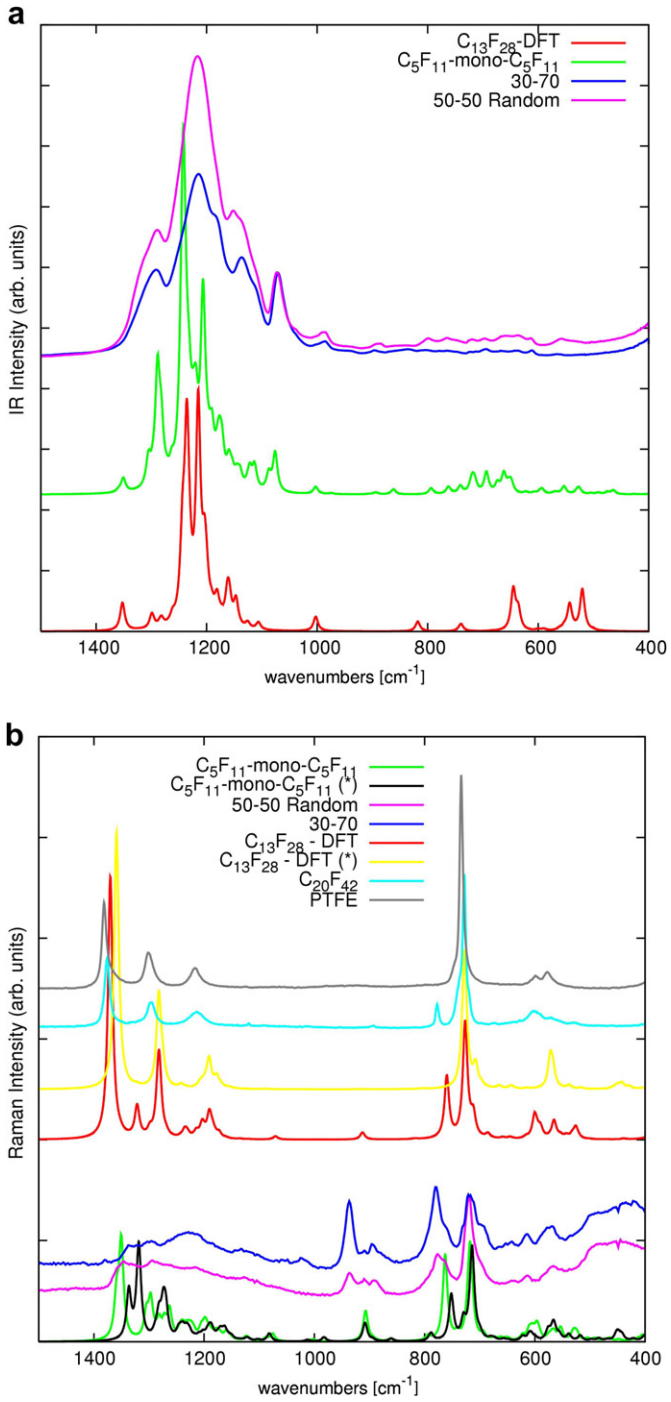

Fig. 9. (a) Comparison between the IR spectrum computed for a model molecule (in the middle) and the experimental ones obtained for TTD–TFE copolymers at different TTD compositions (top); the IR spectrum computed for a TFE chain is also reported (bottom). (b) The same as (a) for Raman spectra. The experimental Raman spectrum of a PTFE sample and an oligo TFE sample ($C_{20}F_{42}$) is also reported. The spectra labelled with a star (*) indicate the cases in which fictitious heavy masses have been introduced on the CF_3 end groups.

the one at 907 cm^{-1} which are indeed assigned to normal modes with large contribution by ring vibrations. These two lines can be correlated to the experimentally observed bands at 776 cm^{-1} and 936 cm^{-1}, respectively, which are sensitive to the content of dioxole.

According to the relative eigenvectors we verified the presence of a relevant contributions from vibrations localized on the COC groups in the dioxole ring.

A further observation has to be made regarding the line at 763 cm^{-1}: if we look at the computed Raman spectrum of a perfluorinated chain we find a line at about the same frequency (760 cm^{-1}). So, at first sight, it seems that the 763 cm^{-1} line predicted for the copolymer model is not a good marker of the dioxole unit.

However, a new simulation of the Raman spectrum of a perfluorinated chain, where fictitious heavy masses were introduced on the CF_3 end groups (the spectrum is shown in Fig. 9b), clearly indicates that this feature can be attributed to the end units. Therefore, it is absent in the case of PTFE chains or in $(CF_2)_n$ sequences belonging to a copolymer chain. A further proof of the reliability of this interpretation is given by the comparison between the experimental Raman spectrum of a PTFE sample and that of $C_{20}F_{42}$ oligomer. A Raman line at 778 cm^{-1} indeed appears in the latter case and is ascribed to CF_3 end groups.

In Fig. 9b a comparison of the theoretical Raman spectrum of the model copolymer and of its fictitious isomer with heavy end groups is also reported. It can be seen that in this case the decoupling of the vibrations localized on the CF_3 groups only slightly affects the feature at 763 cm^{-1}, which still appears (with a modest frequency shift) in the spectrum. The latter observation can be taken as a final proof that the Raman line observed at 776 cm^{-1} in the spectra of copolymers is a good marker of TTD units.

A last comment on the Raman simulations can be made about the spectral region in the range 1400–1100 cm^{-1}, which shows the appearance of several new bands in going from a PTFE chain to the model copolymer. This agrees with the experimental spectra of the copolymer where a very broad unresolved feature is observed in the same region.

The simulations of the vibrational spectra of our model copolymers can be further used in order to make some observations on the FIR features already commented in Section 3.3.

Calculations on the PTFE model ($C_{13}F_{28}$ chain) in its lower energy conformation (15/7 helix) show a strong band at 290 cm^{-1} which can be immediately correlated to the experimental "regularity" band of the polymer at 293 cm^{-1}. The simulated spectrum of our copolymer model shows the appearance of many other FIR features and, in particular, of a quite relevant feature at 250 cm^{-1}. This band could be correlated with the "disorder" band observed at 277 cm^{-1} in the copolymer samples at low TTD concentration.

Similarly the new IR features predicted slightly above 400 cm^{-1} can be correlated to the broad band observed between 380 cm^{-1} and 400 cm^{-1}, which increases with the content of the TTD units.

As already stated in Section 3.2, the use of "disorder" markers (i.e. R_{FIR}) is so far restricted to cases with a low content of TTD units. For this reason the previous observations can be taken only as a very preliminary indication. Sounder conclusions could be obtained by carrying out simulations on more realistic models, as for instance a dioxole unit linked to two long $(CF_2)_n$ chains.

4.2. Conformations

In this last section we present the results of semiempirical simulations which allow to consider more realistic molecular models and also a very large number of equilibrium conformation. The latter point is essential in order to obtain information about the degree of conformational disorder associated with a given chemical structure and to obtain some hints on the flexibility of the molecular chains.

Starting from the molecular structures illustrated in Fig. 5, we explored all the "acceptable" molecular conformations (corresponding to minima of the intramolecular potential energy) obtained by a systematic change of torsional angles ($0-2\pi$ range). Since the number of stable conformers that can be obtained in the case of flexible long chains is very large, we restricted our investigation to the 9 torsional degrees of freedom belonging to the most central units of our models. In the case of the copolymers (*anti* and *syn* models) these 9 degrees of freedom include also the torsional angle of the OCF_3 pendant group. The investigation involves a sequence of logical steps:

1. Definition of a "starting" equilibrium conformation for each molecule. This has been done by performing AM1 optimization on an initial guess geometry. The obtained structures were:
   - PE model (hereafter referred as AM1-PE): all *trans* conformation ($\theta_i = 180°$, for any *i*-th CC bond) of the chain;
   - PTFE model (AM1-PTFE): helical conformation ($\theta_i \sim 167°$, very close to the 15/7 helix structure of the real crystalline polymer);
   - TTD−TFE copolymer model (AM1-copolymer): the structure is similar to that obtained by DFT optimization of the small co-polymer model (Fig. 4(iii)) in the middle of the molecule (i.e. for the dioxole unit and for the adjacent (CF_2CF_2) moieties). The other torsional angles along the two PTFE chains show similar conformation as the AM1-PTFE model. Both *syn* and *anti* configurations were considered.
   - CF_2=CFOCF_3−TFE (MVE−TFE) copolymer model (AM1-copolymer OCF_3): the conformation of the perfluorinated chains is very similar to that in the AM1-copolymer model (*anti* configuration); this model has been introduced in order to test the sensitivity of our calculations to the introduction of co-monomers with a different degree of flexibility.
2. Construction of new geometries by systematic changes of the 9 selected torsional angles. This has been done starting from the geometries obtained at point 1 and increasing any θ_i by finite steps of $\Delta\theta_i = 120°$.[1] Therefore, the possible combinations of the θ_i values give a set of $3^8 \times 6$ different starting geometries for each model.
3. Among these $3^8 \times 6$ geometries, those which are strongly unfavoured by virtue of the steric hindrance of some chemical group were excluded. This selection has been done on the basis of the distance between the non-bonded pairs of atoms (structures showing distances closest than the minimum van der Waals contacts were rejected). This procedure is the same as illustrated in Ref. [36].
4. The final sets of "acceptable" geometries obtained at point 3 were used as input geometries for complete AM1 optimisation. In this way AM1 equilibrium geometries and molecular energies were obtained.

Different possibilities can occur after optimization:

i. The optimized structure shows values of the torsional angles close to those of the input geometry. This means that the calculation has found a minimum "near" the input conformation.
ii. The optimized geometry shows a marked rearrangement of the input $\{\theta_i\}$ values. This indicates that there is no relative minimum of the intramolecular potential energy near the input geometry. In this case the final optimized geometry often corresponds to a minimum which can be reached also starting from a different input geometry.

The "flexibility" of a molecule can be expressed in terms of the number of different equilibrium conformations available, their energies and the height of the potential energy barriers between them. Accordingly, these properties can be investigated through the analysis of the number of conformers and of their energies.We expect the following results:

- With respect to a PE chain, a PTFE chain should show a lower flexibility. In other words the effect of the correlation between adjacent conformational angles is expected to induce a tendency to form helical structures. On the opposite side this effect is not expected in the case of PE, whose structure (in disordered phases) is well described in terms of a statistical coil, made by random sequences of *gauche* and *trans* torsional angles.
- The introduction of a rigid bulky group between two $(CF_2)_n$ chains is expected to decrease the flexibility of the perfluorinated chains, due to the enhancement of the torsional energy barriers caused by the sterical hindrance.

4.2.1. Conformers of polymethylene and polytetrafluoroethylene

In Fig. 10 we report a plot of the conformational energies obtained for AM1-PE and AM1-PTFE models. The conformers have been ordered according to their energy and the value of the abscissa indicates the "order number" of a given structure.The following observations can be made:

- The total number of "acceptable" input geometries is four times larger in the case of PE: this can be simply explained considering that there are many more "rejected conformations" in

[1] Notice that for the torsional angle of the OCF_3 pendant group a finer step, namely $\Delta\theta = 60°$, has been chosen.

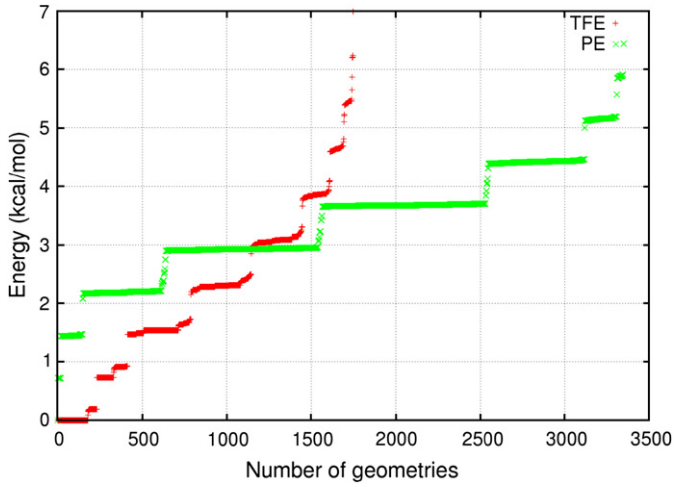

Fig. 10. AM1 conformational energies (kcal/mol) relative to the absolute minimum of the intramolecular potential energys. Green symbols: stable isomers of the AM1-PE model; red symbols: stable isomers of the AM1-PTFE model. (For interpretation of the references to colour in this figure legend, the reader is referred to the web version of this article.)

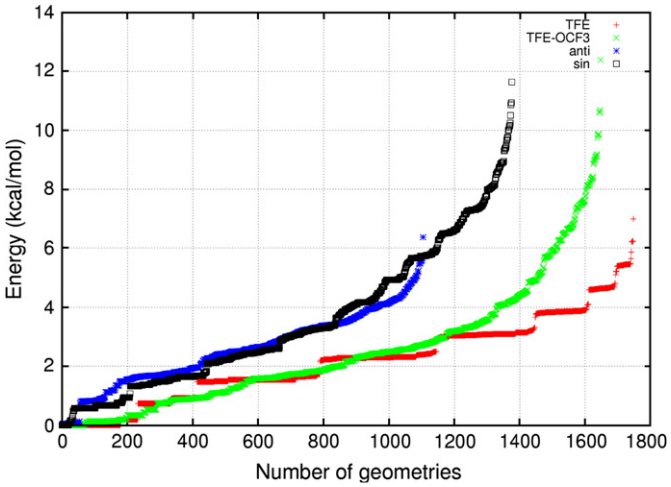

Fig. 11. AM1 conformational energies (kcal/mol) relative to the absolute minimum of the intramolecular potential energy. Blue symbols: stable isomers of AM1-copolymer (*anti*); black symbols: stable isomers of AM1-copolymer (*anti*); green symbols: stable isomers of AM1-copolymer (OCF3) AM1-PE model; red symbols: stable isomers of the AM1-PTFE model. (For interpretation of the references to colour in this figure legend, the reader is referred to the web version of this article.)

the case of PTFE. This is due to the larger van der Waals radius of fluorine with respect to hydrogen.

- In the case of AM1-PTFE, we found many "acceptable" input geometries (178) which "relax" at the lowest energy value. All these species correspond to the same structure, namely the 15/7 helix. This behaviour is markedly different from that shown by PE, where just one starting geometry (namely the *trans*-planar one) results in the fully *trans* optimized structure. We can state that in PTFE the introduction of conformational defects is disfavoured with respect to the helix structure. On the other hand, a PE chain is willing to accommodate local conformational defects.
- Conformers of AM1-PE are grouped by energy steps: the energy values are determined by the total number of *gauche* torsional angles in the conformer and are practically independent of the location of these angles along the chain. This is in good agreement with a simplified picture which assigns a contribution of about 0.5 kcal/mol for each *gauche* torsional angle, independently from its position. The case of AM1-PTFE is quite different: in this case energy steps correspond to conformations which can be always described as short helix sequences.

All the above observations are fully in agreement with what was expected.

4.2.2. Conformers of the copolymers

Let us now consider the case of AM1-copolymer illustrated in Fig. 11. We can see that for both AM1-copolymer (*syn*) and AM1-copolymer (*anti*) the number of "acceptable" input geometries is reduced with respect to the case of PTFE.Some other observations can be made:

- The plots obtained for TTD–TFE copolymers show a steeper increase with respect to that of PTFE, thus indicating that the energy cost to accommodate conformational defects is higher in the case of the copolymer.
- The characteristic grouping of conformers by energy steps (already commented for PE and PTFE models) is not found in the case of copolymers. This behaviour indicates that most of the initial geometries give rise to a characteristic optimized structure, corresponding to a specific local energy minimum, near to the starting structure. This behaviour suggests the presence of high energy barriers, due to the bulky TTD. These barriers do not allow a relaxation of the initial geometry into structures showing large deviations from the initial values of the torsional angles.
- The same effect illustrated above is certainly responsible for the disappearance of the large population corresponding to the lowest energy value which has been observed for AM1-PTFE. The tendency to relax into the regular helix structure is indeed strongly depressed by the introduction of the cyclic co-monomer.

All the above observations can be nicely correlated to the well known effects obtained by co-polymerisation with TTD, namely:

- The decrease of flexibility can be correlated to the reduction of the numbers of "acceptable" input geometries and to the increase of the energy barriers. This last effect implies a reduction of the dynamical flexibility, that is the capability of the chain to overcome these energy barriers, thus increasing the value of T_g.
- The increase of disorder can be correlated to the presence of conformers characterized by different and unique geometries and energies.

We can now compare the behaviour of our models of TTD–TFE copolymers with that predicted for AM1-copolymer

(OCF3). It is clear from Fig. 11 that its behaviour is very similar to that of AM1–TFE, namely that the monomer unit added does not perturb to a great extent on the number and the energies of the available conformations.

This clearly confirms that the extent of the ''perturbation'' is crucially determined by the chemical structure and conformation of the added co-monomer.

5. Conclusions

The analysis presented in this work allows to rationalize, at the molecular level, the effect of the co-polymerisation of TFE with a bulky chemical group. The presence of TTD units *prevents the formation of crystalline phases* through several different actions:

1. The introduction of chemical, configurational and conformational *local* disorder in the polymer chain is obviously responsible for a decrease of crystallinity. The interesting point is that a TTD unit seems to perturb the structure of the chain to a greater extent with respect to other (less bulky) chemical defects. This conclusion is supported by AM1 studies on the stable conformational isomers of models of PTFE, TFE–TTD copolymer and MVE–TFE copolymer. Moreover, spectroscopic signals attributed to ''disordered'' TFE sequences can be clearly detected in the FIR spectra of copolymers with low TTD content and are nicely reproduced by DFT simulations.
2. High energy barriers in the potential energy upon variation of the torsional degrees of freedom cause a decrease of the chain flexibility. This effect (clearly suggested by the AM1 study) is due to the steric hindrance of TTD units and can slow down or even prevent the crystallisation process for TFE sequences.

Point 2 also explains why the copolymers show high glass transition temperatures.

From the side of the structural characterisation, we have shown that the joint use of experiments (IR and Raman spectra) and spectra simulations (obtained by high level DFT calculations on small molecular models) allows to identify frequency markers correlated to the presence of TTD units and to verify the sensibility of several bands to the different configurations of the TFE units attached to the ring.

References

[1] Scheirs J, editor. Modern fluoropolymers: high performance polymers for diverse applications. New York: John Wiley and Sons, ISBN 978-0-471-97055-2; 1997.
[2] Wlassics I, Tortelli V. J Fluorine Chem, in press. doi:10.1016/j.jfluchem.2008.01.018.
[3] Hougham G, et al., editors. Fluoropolymers: synthesis and properties, vol. II. New York: Plenum Press; 1999.
[4] Resnick PR. J Fluorine Chem 1989;45(1):100.
[5] Legeay G, Coudreuse A, Legais JM, Werner L, Bulou A, Buzare JY, et al. Eur Polym J 1998;34(10):1457–65.
[6] Leitz M, Podgorsek RP, Franke H, Hernandez D, Knystautas EJ, Lessard RA. Opt Eng 2001;40(7):1315–20.
[7] Altkorn R, Koev I, Van Duyne RP, Litorja M. Appl Opt 1997;36(34):8992–8.
[8] Smart BE, Feiring AE, Krespan CG, Zhen Y, Ming H, Resnick PR, et al. Macromol Symp 1995;98:753.
[9] Afonina II, Nevezhina TB, Andreeva AI, Zaichenko YA, Sannikov SG, Ostrizhko FN, et al. Int Polym Sci Tech 1996;23:44.
[10] Chen GF, Xia ZF, Zhang YW, Zhang HY. IEEE T Dielect El In 1999;6:381.
[11] Yamamoto K, Ogawa G. J Fluorine Chem 2005;126(9–10):1403–8.
[12] Mikes F, Yang Y, Teraoka I, Ishigure T, Koike Y, Okamoto Y. Macromolecules 2005;38(10):4237–45.
[13] Sasaki K, Kawamura N, Tokumaru H, Sakane Y. Appl Phys Lett 2004;85(7):1134–6.
[14] Russo A, Navarrini W. J Fluorine Chem 2004;125(1):73–8.
[15] Apostolo M, Triulzi F, Arcella V, Calini P. Patent EP1256592 A1; 2002.
[16] Russo A, Navarrini W. US Patent 6,335,408 B1; 2002.
[17] Apostolo M, Triulzi F, Arcella V. Patent EP1469016A1; 2004.
[18] Colaianna P, Brinati G, Arcella V. US Patent 5,883,177; 1999.
[19] Navarrini W, Tortelli V, Zedda A. US Patent 5,589,557 A; 1996;
Navarrini W, Tortelli V. US Patent 5,495,028; 1996;
Navarrini W, Fontana S. US Patent 5,296,617 A; 1994;
Navarrini W, Bragante L, Fontana S, Tortelli V, Zedda A. J Fluorine Chem 1995;71(1):111–7.
[20] Arcella V, Apostolo M, Triulzi F. Patent EP1469015A1; 2004.
[21] Arcella V, Brinati G, Maccone P. US Patent 6,072,020; 2000;
Arcella V, Colaianna P, Maccone P, Sanguineti A, Giordano A, Clarizia G, et al. J Membr Sci 1999;163(2):203–9.
[22] Groh W. Makromol Chem 1988;189(12):2861–74.
[23] Califano S. Vibrational states. London: John Wiley and Sons; 1976.
[24] Wilson EB, Decius JC, Cross PC. Molecular vibrations: the theory of infrared and Raman vibrational spectra. New York: McGraw-Hill; 1955.
[25] Zerbi G, Sacchi M. Macromolecules 1973;6(5):692–9.
[26] Tadokoro H. Structure of crystalline polymers. New York: Wiley; 1979.
[27] Moynihan RE. J Am Chem Soc 1959;81(5):1045–50.
[28] De Santis P, Giglio E, Liquori AM, Ripamonti A. J Polym Sci Part A 1963;1:1383.
[29] Rabolt JF, Fanconi B. Macromolecules 1978;11(4):740–5.
[30] Rabolt JF. J Polym Sci Polym Phys Ed 1983;21(9):1797–805.
[31] Masetti G, Cabassi F, Morelli G, Zerbi G. Macromolecules 1973;6(5):700–7.
[32] Colaianna P, Abusleme J. Patent EP0720992 A1; 1996;
Navarrini W, Tortelli V. Patent EP0633257 A1; 1995.
[33] Becke AD. J Chem Phys 1993;98(7):5648–52.
[34] Dewar MJS, Zoebisch EG, Healy EF, Stewart JJP. J Am Chem Soc 1985;107(13):3902–9.
[35] Radice S, Tortelli V, Causà M, Castiglioni C, Zerbi G. J Fluorine Chem 1999;95(1–2):105–16.
[36] Tommasini M, Castiglioni C, Milani A, Zerbi G, Radice S, Toniolo P, et al. J Fluorine Chem 2006;127(3):320–9.